

## EVOLVING SPIKING NEURAL NETWORK TOPOLOGIES FOR BREAST CANCER CLASSIFICATION IN A DIELECTRICALLY HETEROGENEOUS BREAST

M. O'Halloran<sup>1, 2, \*</sup>, S. Cawley<sup>1, 2</sup>, B. McGinley<sup>1, 2</sup>,  
R. Conceicao<sup>1, 2</sup>, F. Morgan<sup>1, 2</sup>, E. Jones<sup>1, 2</sup>, and M. Glavin<sup>1, 2</sup>

<sup>1</sup>College of Engineering and Informatics, National University of Ireland Galway, University Road, Galway, Ireland

<sup>2</sup>Bioelectronics Research Cluster, National Centre for Biomedical Engineering Science (NCBES), National University of Ireland Galway, University Road, Galway, Ireland

**Abstract**—Several studies have investigated the possibility of using the Radar Target Signature (RTS) of a tumour to classify the tumour as either benign or malignant, since the RTS has been shown to be influenced by the size, shape and surface texture of tumours. The Evolved-Topology Spiking Neural Neural (SNN) presented here extends the use of evolutionary algorithms to determine an optimal number of neurons and interneuron connections, forming a robust and accurate Ultra Wideband Radar (UWB) breast cancer classifier. The classifier is examined using dielectrically realistic numerical breast models, and the performance of the classifier is compared to an existing Fixed-Topology SNN cancer classifier.

### 1. INTRODUCTION

In the United States alone, breast cancer accounts for 31% of new cancer cases, and is second only to lung cancer as the leading cause of deaths in American women [1]. The current standard screening method for detecting non-palpable early stage breast cancer is X-ray mammography. Despite the fact that X-ray mammography provides high resolution images using relatively low radiation doses, its limitations are well documented [2]. The search for new imaging

---

*Received 6 May 2011, Accepted 27 July 2011, Scheduled 8 August 2011*

\* Corresponding author: Martin O'Halloran (martin.ohalloran@gmail.com).

techniques is motivated by the need for increased specificity and sensitivity, especially in the case of radiographically dense tissue.

One of the most promising emerging breast imaging modalities is UWB Radar imaging. The physical basis of UWB Radar imaging is the dielectric contrast between normal and malignant breast tissue that exists at microwave frequencies [3–8].

This dielectric contrast is due to the increased water content present in the cancerous tissue, and this contrast ensures that when the breast is illuminated by an Ultra Wideband (UWB) pulse, cancerous tissue in the breast tissue will provide backscattered energy, which may be used to detect, localise and classify tumours. UWB Radar imaging is non-ionising, non-invasive, does not require uncomfortable breast compression, and is potentially lower cost.

Several studies have also examined the use of UWB Radar to classify breast cancer. This classification approach is based on the Radar Target Signature, which reflects the size, shape and surface texture of the tumour. Benign tumours typically have smooth surfaces and have spherical, oval or at least well-circumscribed contours. Conversely, malignant tumours usually present rough and complex surfaces with spicules or microlobules, and their shapes are typically irregular, ill-defined and asymmetric [9]. These tumour characteristics are generally reflected in the details of the RTS and can be used in classifiers. Several classifiers and classification architectures have been investigated [10–15].

In this paper, a novel Spiking Neural Network (SNN) classifier is presented and examined. SNNs [16] emulate biological neurons and aim to replicate the brains ability to function well when presented with noisy or incomplete data. SNNs are typically trained for a specific task using a Genetic Algorithm (GA), a type of evolutionary algorithm. This training process involves modifying neuron firing thresholds and synaptic weights. This paper extends the use of evolutionary algorithms to determine an optimal number of neurons and interneuron connections to form a UWB breast cancer classifier. This approach results in networks which are more compact than traditional fixed topology networks and simplifies the search space resulting in faster training time and increased accuracy.

The structure of the paper is as follows: Section 2 describes the SNNs and the NEAT Genetic Algorithm used for SNN training; Section 3 describes the generation of realistic tumour models, including dielectric heterogeneity and corresponding FDTD simulations; while Section 4 describes the results and Section 5 draws the corresponding conclusions.

## 2. SPIKING NEURAL NETWORKS AND EVOLVING TOPOLOGIES

### 2.1. Spiking Neural Network

Spiking Neural Networks (SNNs) are more closely related to their biological counterparts than previous Artificial Neural Networks (ANNs) generations, such as multi-layer perceptrons. SNNs, in contrast to previous models, employ transient pulses for communication and computation. Maass has demonstrated that spiking neurons are more computationally powerful than threshold-based neuron models [16] and that SNNs possess similar and often more computation ability compared to multi-layer perceptrons [17].

Inspired by nature, a Genetic Algorithm (GA) [18] models natural evolution through a set of computational operators. A GA is a parallel, population-based search strategy that encodes individual solutions into a data-structure known as a genome. A population of such genomes is maintained by the GA and mechanisms analogous to evolution are employed to evolve high-fitness solutions. Exploration of the search space is performed using a diversity introducing mutation operator while crossover (mating of two parent solutions) is employed to exploit good solution building blocks (known as genes) already in the population. Selection pressure is added through a tournament selection operator to incorporate “survival of the fittest”. Traditionally SNN simulations involve constructing a fixed, regular structure of neurons arranged in layers where all neurons are fully-forward connected (Figure 1). This approach simplifies the design of the network and provides a structure whose neuron firing thresholds and synaptic interconnect weights may be evolved, with a fixed-length genome, to

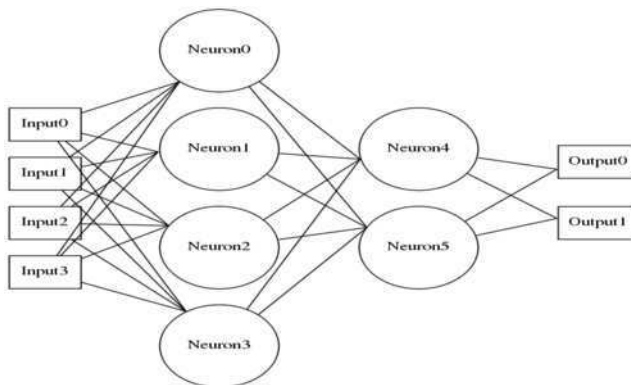


**Figure 1.** Example fixed-topology spiking neural network.

form a solution. Recently, there has been growing interest in exploiting the adaptability provided by GAs to modify the interconnect structure of an SNN in order to create a topology which is both simpler and more suitable for the task at hand. A common issue with this concept is designing an appropriate encoding mechanism for the structure of the network such that it may be mutated and combined with other networks in a feasible manner. Additionally network structures evolved by a GA have a tendency to grow as the GA progresses. This topology growth results in a more complex search space partly negating the advantage of evolving a task specific network.

The authors have chosen to incorporate the NeuroEvolution through Augmenting Topologies (NEAT) [19] algorithm which is tailored to address these particular concerns. The NEAT algorithm incorporates historical markers in the SNN gene which allows genes with common ancestors to be combined as part of the GA's crossover mechanism. NEAT also uses this historical information to group individuals into species based on common ancestors [19]. When the GA creates a new generation, selection of individuals (i.e., choosing which individuals will be combined together to form an individual for the new population) is traditionally based on each individual's fitness. NEAT implements explicit fitness sharing [20] within species, where individuals in a species must share their combined fitness (i.e., the fitness of an individual is modified to be the average fitness of all individuals in that species). This deters species from growing too large, as each individual must contribute to the species fitness, hence allowing many diverse species (i.e., many unique approaches to solving the problem) to co-exist. Species whose fitness does not increase over a number of generations become extinct (i.e., the individuals are deleted from the population and replaced with new, randomly-initialized, individuals) ensuring individuals continue to improve as the network complexity grows. Traditional fully connected SNNs will contain many neurons and connections which do not contribute to classifier accuracy. The NEAT operators create networks which are of optimal size and only contain neurons and connections which aid the function of the classifier.

## 2.2. Preprocessing and Fitness Function

The classifier considered here is a two-class problem (i.e., malignant vs. benign). The Discrete Wavelet Transform (DWT) is applied to extract the most significant classification features of the RTS, in a process previously described more comprehensively in [21]. In this study, large DWT values are mapped to high spike frequencies while small DWT values are mapped to low frequencies. Since values are scaled between

$[-1, +1]$ , it is necessary to decouple the positive and negative ranges of each DWT component ( $D(n)$ ) into two spike generating inputs ( $D(n)+$  and  $D(n)-$ ). This decoupling ensures that a  $+1$  DWT input generates the same number of spikes (and influence) on the SNN as a  $-1$  DWT input, thus removing any bias from the encoding process. The SNN processes the 15 most significant DWT components. Thirty spike generators are used to map real-valued DWT data into spike trains using a linear magnitude to (spike train) frequency conversion [22].

Two output layer spiking neurons generate two spike trains, which are processed by two spike counters to count the number of output spikes within a given update interval [22]. These counter values are used to determine classifier behaviour. The counter with the largest spike count value designates the selected class. The neuron model chosen for these experiments is based on the leaky integrate and fire model [16]. Each SNN individual is initially composed of thirty input neurons and two output neurons. The NEAT GA progressively adds neurons and connections and hence each individual has a variable number of genes. The GA also modifies the weights on the synaptic connections and neuron firing threshold.

Synaptic weights range from  $[-1, 1]$  while thresholds vary between  $[0, 5.0]$  [23]. Fitness assessment of the SNN-based breast cancer classifier is achieved using a fitness function, which rewards individuals based on the number of correct classifications made.  $C_m$  refers to the number of correct malignant classifications made by the SNN.  $C_b$  refers to the number of correct benign classifications.  $C_{\max}$  and  $C_{\min}$  are defined in Equations (2) and (3). The fitness function,  $f$ , of the SNN is defined as follows:

$$f = C_{\min}\beta + C_{\max} \quad (1)$$

where

$$C_{\max} = \max(C_m, C_b) \quad (2)$$

$$C_{\min} = \min(C_m, C_b) \quad (3)$$

A  $\beta$  value of 1.6, chosen through empirical analysis, is employed in this research to reward the correct classification of both tumour classes. Without this fitness bias, fitness can be accumulated by classifying a single tumour class repeatedly. By including a  $\beta$  value greater than one, networks that select correctly from both classes are rewarded above networks that correctly select from just one class.

### 3. BREAST AND TUMOUR MODELING

Shape and texture of the surface of a tumour are two of the most important characteristics used to differentiate between a benign and

a malignant tumour. The tumour models used in this paper are based on the Gaussian Random Spheres (GRSs) method [24, 25]. Three different tumour models at two different sizes are considered in this paper. Malignant tumours are represented by spiculated and microlobulated GRSs, whereas benign tumours are modelled by smooth GRSs. Microlobulated and smooth GRSs are obtained by varying the correlation angle from low to high. Spiculated GRSs are obtained by adding 3, 5 or 10 spicules to smooth GRSs. The average radius of all types of spheres are 2.5 and 7.5 mm. Between all sizes and shapes, the number of tumour models developed was 160 (80 malignant and 80 benign). Two sets of simulations were performed to examine performance in heterogenous tissue. For the first set (Hetero I), a single piece of fibroglandular tissue is added to the FDTD models, positioned at one of ten random locations surrounding the tumour. For the second set of simulations (Hetero II), two independent portions of fibroglandular tissue are positioned at two of ten random locations around the tumour. Portions of fibroglandular tissue were extracted from the UCWEM Breast Phantom Repository (phantom ID 071904). The background material is assumed to be homogeneous adipose tissue. In order to model loss and dispersion, the dielectric properties of adipose, fibroglandular and cancerous tissue are modelled using Debye parameters based on the dielectric data as published by Lazebnik et al. [7, 8].

The tumours (80 of size 2.5 mm and 80 of size 7.5 mm) are placed in a 3D Finite-Difference Time-Domain (FDTD) model. The FDTD model has a 0.5 mm cubic grid resolution and the backscattered signals were generated through a Total-Field/Scattered-Field (TF/SF) structure, in which the tumours and fibroglandular tissue are completely embedded in the Total Field (TF) [13, 15]. A pulsed plane wave is transmitted towards the target from four different equidistant angles ( $0^\circ, 90^\circ, 180^\circ, 270^\circ$ ) and the resulting cross-polarized backscatter is recorded and analyzed from four observation points located at:  $(0, 0, -74)$ ,  $(-74, 0, 0)$ ,  $(0, 0, 74)$  and  $(74, 0, 0)$  mm in  $(x, y, z)$  axes. The incident pulse is a modulated Gaussian pulse with center frequency at 6 GHz where the  $1/e$  full temporal width of the Gaussian envelope was 160 ps. A more detailed description of both the tumours and the model is presented in [21].

#### 4. RESULTS

In this study, a direct “type” classifier that simply classifies each tumour as either benign or malignant is considered. The tumour backscatter is classified using the Evolved-Topology SNN presented

**Table 1.** Comparison of fixed and evolved-topology SNN classifiers.

Classifier	One-Stage Type (%)
Fixed-Topology SNN	73
Evolved-Topology SNN	83

**Table 2.** Effects of dielectric heterogeneity on performance of SNN classifiers. Hetero I refers to models containing one piece of fibroglandular tissue, while Hetero II refers to models with two pieces of fibroglandular tissue.

Classifier	Hetero I (%)	Hetero II (%)
Fixed-Topology SNN	78	68
Evolved-Topology SNN	86.75	79.4

here, but also using a Fixed-Topology SNN previously presented by the authors [21], providing a useful baseline when examining the performance and robustness of the Evolved-Topology SNN classifier. In order to evaluate both classification methods, the entire data-set is randomly shuffled and divided into 75% (120 Tumours) and 25% (40 Tumours) training and test groups respectively. The classification process is repeated 10 times and the average performance of each classifier is calculated. The results are presented in Table 1 and illustrate a 10% increase in accuracy for the Evolved-Topology SNN compared to the traditional fixed topology SNN.

#### 4.1. Effects of Dielectric Heterogeneity

In order to examine the effect of increasing dielectric heterogeneity on the performance of the SNN classifier, two specific scenarios are considered. In the first instance, a single piece of fibroglandular tissue surrounds the tumour, while in the second more difficult scenario two separate pieces of fibroglandular tissue are located around the tumour. The performance of the classifier in an increasingly heterogeneous environment is shown in Table 2. The performance of the classifiers drops by 10% and 7.4% for one-stage type for the traditional and Evolved-Topology SNN respectively as heterogeneity increases. Overall, the Evolved-Topology SNN classifier is shown to be relatively robust to significant increases in dielectric heterogeneity. In fact, in the most dielectrically heterogeneous models (Hetero II), the average performance (across large and small tumours) of the Evolved-Topology SNN classifier was almost 80%.

## 5. CONCLUSION

The performance of an Evolved-Topology SNN based classifier (based on the NEAT algorithm) in a dielectrically heterogeneous breast was examined in this paper and compared to the performance of a traditional fixed topology SNN. Results demonstrate the ability of Evolved-Topology SNN classifiers to outperform a traditional SNN classifier. The improved classification performance can be attributed to the following:

- Specialisation within the GA population allows differing approaches to solving the task to evolve in parallel, effectively protecting potential innovative network structures and forcing search within many solution spaces to proceed in parallel.
- Historical markers inserted into each individual's genes by NEAT allows divergent networks to be combined in an intelligent manner. This feature allows different networks which have, for example, evolved to perform well on a particular size of tumor to be combined in a manner which preserves and combines each networks specialisation.
- Finally, as NEAT promotes minimal networks, the search space remains small allowing for a greater exploration of the search space.

## ACKNOWLEDGMENT

This work is supported by Science Foundation Ireland (SFI) under grant numbers 07/RFP/ENEF420 and 07/SRC/I1169 and the Irish Research Council for Science, Engineering and Technology (IRCSET).

## REFERENCES

1. Dixon, M. J., *ABC of Breast Diseases*, Wiley-Blackwell, 2006.
2. Nass, S. L., I. C. Henderson, and J. C. Lashof, *Mammography and Beyond: Developing Technologies for the Early Detection of Breast Cancer*, National Academy Press, 2001.
3. Chaudhary, S. S., R. K. Mishra, A. Swarup, and J. M. Thomas, "Dielectric properties of normal and malignant human breast tissue at radiowave and microwave frequencies," *Indian J. Biochem. Biophys.*, Vol. 21, 76–79, 1984.
4. Surowiec, A. J., S. S. Stuchly, J. R. Barr, and A. Swarup, "Dielectric properties of breast carcinoma and the surrounding



- tissues,” *IEEE Trans. Biomed. Eng.*, Vol. 35, No. 4, 257–263, Apr. 1988.
5. Joines, W. T., Y. Zhang, C. Li, and R. L. Jirtle, “The measured electrical properties of normal and malignant human tissues from 50 to 900 MHz,” *Med. Phys.*, Vol. 21, No. 4, 547–550, Apr. 1994.
  6. Campbell, A. M. and D. V. Land, “Dielectric properties of female human breast tissue measured in vitro at 3.2 GHz,” *Phys. Med. Biol.*, Vol. 37, No. 1, 193–210, 1992.
  7. Lazebnik, M., L. McCartney, D. Popovic, C. B. Watkins, M. J. Lindstrom, J. Harter, S. Sewall, A. Magliocco, J. H. Booske, M. Okoniewski, and S. C. Hagness, “A large-scale study of the ultrawideband microwave dielectric properties of normal breast tissue obtained from reduction surgeries,” *Phys. Med. Biol.*, Vol. 52, 2637–2656, 2007.
  8. Lazebnik, M., D. Popovic, L. McCartney, C. B. Watkins, M. J. Lindstrom, J. Harter, S. Sewall, T. Ogilvie, A. Magliocco, T. M. Breslin, W. Temple, D. Mew, J. H. Booske, M. Okoniewski, and S. C. Hagness, “A large-scale study of the ultrawideband microwave dielectric properties of normal, benign and malignant breast tissues obtained from cancer surgeries,” *Phys. Med. Biol.*, Vol. 52, 6093–6115, 2007.
  9. Nguyen, M. and R. Rangayyan, “Shape analysis of breast masses in mammograms via the fractal dimension,” *IEEE Engineering in Medicine and Biology 27th Annual Conference*, 3210–3213, 2005.
  10. AlShehri, S. A., S. Khatun, A. B. Jantan, R. S. A. Raja Abdullah, R. Mahmood, and Z. Awang, “3D experimental detection and discrimination of malignant and benign breast tumor using nn-based UWB imaging system,” *Progress In Electromagnetics Research*, Vol. 116, 221–237, 2011.
  11. Conceicao, R. C., M. O’Halloran, M. Glavin, and E. Jones, “Effects of dielectric heterogeneity in the performance of breast tumour classifiers,” *Progress In Electromagnetics Research M*, Vol. 17, 73–86, 2011.
  12. Conceicao, R. C., M. O’Halloran, M. Glavin, and E. Jones, “Evaluation of features and classifiers for classification of early-stage breast cancer,” *Journal of Electromagnetic Waves and Applications*, Vol. 25, No. 1, 1–14, 2011.
  13. Conceicao, R. C., M. O’Halloran, E. Jones, and M. Glavin, “Investigation of classifiers for early-stage breast cancer based on radar target signatures,” *Progress In Electromagnetics Research*, Vol. 105, 295–311, 2010.

14. Conceicao, R. C., M. O'Halloran, M. Glavin, and E. Jones, "Support vector machines for the classification of early-stage breast cancer based on radar target signatures," *Progress In Electromagnetics Research B*, Vol. 23, 311–327, 2010.
15. Davis, S. K., B. D. V. Veen, S. C. Hagness, and F. Kelcz, "Breast tumor characterization based on ultrawideband backscatter," *IEEE Trans. Biomed. Eng.*, Vol. 55, No. 1, 237–246, 2008.
16. Maass, W., "Networks of spiking neurons: The third generation of neural network models," *Neural Networks*, Vol. 10, No. 9, 1659–1671, 1997.
17. Maass, W., "Computing with spiking neurons," *Pulsed Neural Networks*, 85, MIT Press, 1999.
18. Holland, J., *Adaptation in Natural and Artificial Systems*, MIT Press, Cambridge, MA, 1992.
19. Stanley, K. O. and R. Miikkulainen, "Evolving neural networks through augmenting topologies," *Evolutionary Computation*, Vol. 10, No. 2, 99–127, Jun. 2002.
20. Goldberg, D. and J. Richardson, "Genetic algorithms with sharing for multimodal function optimization," *Proceedings of the Second International Conference on Genetic Algorithms and Their Application*, 41–49, 1987.
21. O'Halloran, M., B. McGinley, R. C. Conceicao, F. Morgan, E. Jones, and M. Glavin, "Spiking neural networks for breast cancer classification in a dielectrically heterogeneous breast," *Progress In Electromagnetics Research*, Vol. 113, 413–428, 2011.
22. Pande, S., F. Morgan, C. Seamus, B. Mc Ginley, S. Carrillo, L. McDaid, and J. Harkin, "EMBRACE-sysC for analysis of NoC-based spiking neural network architecture," *IEEE System on a Chip Symposium (SOC)*, 2010.
23. Roche, P., B. McGinley, J. Maher, F. Morgan, and J. Harkin, "Investigating the suitability of FPAA's for evolved hardware spiking neural networks," *Proceedings of Evolvable Systems: from Biology to Hardware*, 118–126, 2008.
24. Muinonen, K., "Introducing the gaussian shape hypothesis for asteroids and comets," *Astronomy and Astrophysics*, Vol. 332, 1087–1098, 1998.
25. Mishchenko, M. I., "Light scattering by stochastically shaped particles," *Light Scattering by Nonspherical Particles: Theory, Measurements, and Applications*, Ch. 11, Academic Press, 2000.